Title

Distinct Metabolic States Can Support Self-Renewal and Lipogenesis in Human Pluripotent Stem Cells under Different Culture Conditions

Journal

Cell Reports, 16(6)

ISSN

2639-1856

Authors

Zhang, Hui
Badur, Mehmet G
Divakaruni, Ajit S
et al.

Publication Date

2016-08-01

DOI

10.1016/j.celrep.2016.06.102

Peer reviewed

Article

Cell Reports

Distinct Metabolic States Can Support Self-Renewal and Lipogenesis in Human Pluripotent Stem Cells under Different Culture Conditions

Graphical Abstract

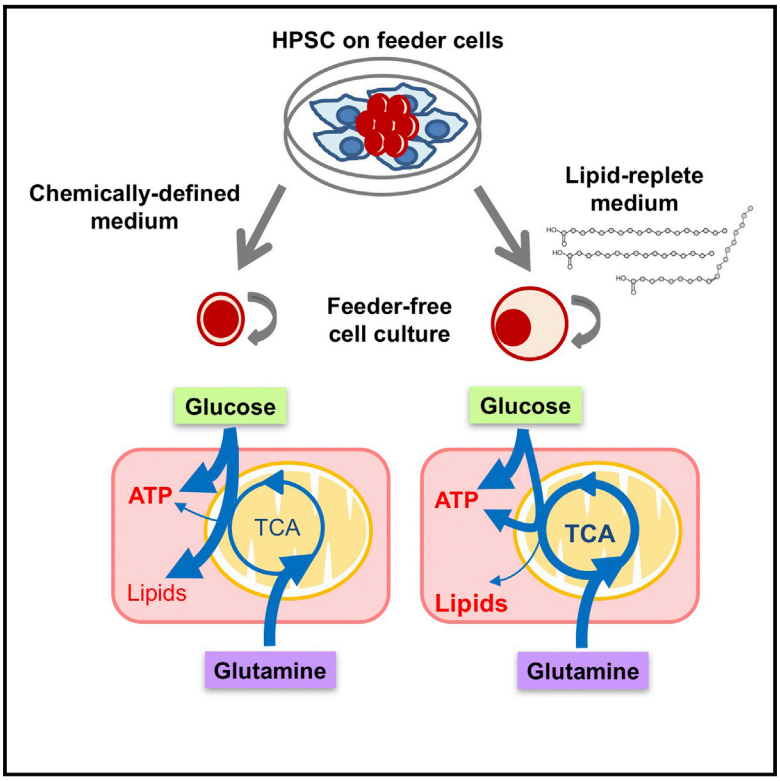

Highlights

- Medium choice influences the metabolic state of hPSCs
- Chemically defined medium reprograms hPSC lipogenic and redox metabolic pathways
- hPSCs cultured in lipid-replete medium exhibit active oxidative mitochondrial flux
- Glutamine fuels mitochondrial metabolism in self-renewing hPSCs

Authors

Hui Zhang, Mehmet G. Badur, Ajit S. Divakaruni, ..., Karsten Hiller, Anne N. Murphy, Christian M. Metallo

Correspondence

cmetallo@ucsd.edu

In Brief

Zhang et al. apply metabolic flux analysis to comprehensively characterize the metabolism of human pluripotent stem cells cultured in different media. Cells maintained in chemically defined media significantly upregulate lipid biosynthesis and redox pathways to compensate for medium lipid deficiency while downregulating oxidative mitochondrial metabolism.

Zhang et al., 2016, Cell Reports *16*, 1–12
August 9, 2016
http://dx.doi.org/10.1016/j.celrep.2016.06.102

CellPress

Please cite this article in press as: Zhang et al., Distinct Metabolic States Can Support Self-Renewal and Lipogenesis in Human Pluripotent Stem Cells under Different Culture Conditions, Cell Reports (2016), http://dx.doi.org/10.1016/j.celrep.2016.06.102

Cell Reports
Article

Distinct Metabolic States Can Support Self-Renewal and Lipogenesis in Human Pluripotent Stem Cells under Different Culture Conditions

Hui Zhang,[1,5] Mehmet G. Badur,[1,5] Ajit S. Divakaruni,[3] Seth J. Parker,[1] Christian Jäger,[4] Karsten Hiller,[4] Anne N. Murphy,[3] and Christian M. Metallo[1,2,*]
[1]Department of Bioengineering, University of California, San Diego, La Jolla, CA 92037, USA
[2]Moores Cancer Center, University of California, San Diego, La Jolla, CA 92037, USA
[3]Department of Pharmacology, University of California, San Diego, La Jolla, CA 92037, USA
[4]Luxembourg Centre for Systems Biomedicine, University of Luxembourg, Belvaux, 4367 Luxembourg
[5]Co-first author
*Correspondence: cmetallo@ucsd.edu
http://dx.doi.org/10.1016/j.celrep.2016.06.102

SUMMARY

Recent studies have suggested that human pluripotent stem cells (hPSCs) depend primarily on glycolysis and only increase oxidative metabolism during differentiation. Here, we demonstrate that both glycolytic and oxidative metabolism can support hPSC growth and that the metabolic phenotype of hPSCs is largely driven by nutrient availability. We comprehensively characterized hPSC metabolism by using $^{13}C/^{2}H$ stable isotope tracing and flux analysis to define the metabolic pathways supporting hPSC bioenergetics and biosynthesis. Although glycolytic flux consistently supported hPSC growth, chemically defined media strongly influenced the state of mitochondrial respiration and fatty acid metabolism. Lipid deficiency dramatically reprogramed pathways associated with fatty acid biosynthesis and NADPH regeneration, altering the mitochondrial function of cells and driving flux through the oxidative pentose phosphate pathway. Lipid supplementation mitigates this metabolic reprogramming and increases oxidative metabolism. These results demonstrate that self-renewing hPSCs can present distinct metabolic states and highlight the importance of medium nutrients on mitochondrial function and development.

INTRODUCTION

Given their virtually unlimited expansion potential and differentiation capacity, human pluripotent stem cells (hPSCs) offer unique opportunities in the study of human development, biochemical screening in specific lineages, and regenerative medicine. Successful establishment of culture conditions able to maintain human embryonic stem cells (hESCs) and induced pluripotent stem cells (iPSCs) in the undifferentiated state represented critical steps in advancing these technologies to practice (Thomson et al., 1998; Takahashi and Yamanaka, 2006). However, the large quantity of cells needed for screening and tissue engineering applications poses a challenge that must still be addressed (Desai et al., 2015). Initial protocols for hPSC self-renewal mimicked the in vivo microenvironment by using feeder cell co-culture or medium conditioned by feeder cells to support hPSC expansion (Villa-Diaz et al., 2013; Desai et al., 2015). However, current good manufacturing practices (cGMPs) and Food and Drug Administration (FDA) guidelines that encourage the use of xenobiotic-free systems in clinical applications of hPSCs have driven efforts to develop chemically defined and/or xenobiotic-free media and substrates for hPSC maintenance (Kirouac and Zandstra, 2008; Hyun et al., 2008; Carpenter and Couture, 2010). In recent years, such chemically defined formulations have supplanted undefined conditions as the gold standard for expansion of hPSCs (Ludwig et al., 2006; Chen et al., 2011). However, the metrics for evaluation of such media have often been limited to proliferation, pluripotency, and gene expression analyses, an established challenge that must still be overcome (Ungrin et al., 2007). Indeed, recent studies now suggest that culture and/or passaging conditions can influence the genetic stability, metabolism, and differentiation potential of hPSCs (Laurent et al., 2011; Badur et al., 2015; Lee et al., 2015). The specific metabolic features of hPSCs adapted to chemically defined media must be elucidated in greater detail to develop improved hPSC models and related biomedical products.

Several recent studies have identified critical metabolic pathways necessary for cellular reprogramming and/or maintaining pluripotency, evoking a broader interest in applying hPSCs to study nutrition, development, and metabolic disease (Ben-Zvi and Melton, 2015). Glycolytic flux is commonly high in hPSC cultures, and inhibition of glucose metabolism potently limits reprogramming efficiency (Folmes et al., 2011; Panopoulos et al., 2012; Zhu et al., 2010). Metabolites that serve as substrates for epigenetic markers such as acetylation and methylation have also emerged as critical regulators of pluripotency (Moussaieff et al., 2015; Shiraki et al., 2014; Wang et al., 2009; Shyh-Chang et al., 2013). Broader characterization of the hPSC metabolome has also identified key differences in mitochondrial function and

Please cite this article in press as: Zhang et al., Distinct Metabolic States Can Support Self-Renewal and Lipogenesis in Human Pluripotent Stem Cells under Different Culture Conditions, Cell Reports (2016), http://dx.doi.org/10.1016/j.celrep.2016.06.102

lipid metabolism between hPSCs, mouse (m)ESCs, and their derivatives (Panopoulos et al., 2012, Yanes et al., 2010). In addition, compounds that promote mitochondrial metabolism can negatively influence cellular reprogramming (Folmes et al., 2011; Panopoulos et al., 2012; Zhu et al., 2010), leading to the generalized concept that oxidative mitochondrial metabolism is ''antagonistic'' to the pluripotent state (Zhang et al., 2012). However, some evidence suggests that mitochondria are active in hESCs (Zhang et al., 2011). Similar to recent developments in tumor biology (Viale et al., 2014), critical roles for mitochondria in hPSC growth are likely to emerge.

Here we conducted a comprehensive analysis of metabolic fluxes in hPSCs. Using an array of ^{13}C and ^{2}H tracers, we investigated the metabolic pathways that support hPSC biosynthesis and growth. Surprisingly, we observed that distinct metabolic states marked by high mitochondrial flux and governed by nutrient availability can maintain hESC self-renewal, challenging the notion that mitochondrial function is dispensable for stem cell function. Chemically defined medium drives hPSCs to regulate mitochondrial pathways to support lipid biosynthesis at the expense of oxidative metabolism. Media containing lipid supplements maintain pluripotency while augmenting respiration and mitochondrial metabolism. Taken together, these results demonstrate that nutrient availability and the microenvironment (in particular, medium choice) profoundly affect hPSC metabolism.

RESULTS

Medium Choice Influences hESC Metabolic States

To define the critical metabolic features of self-renewing hPSCs, we quantified intracellular metabolite abundances, nutrient uptake, and byproduct secretion in undifferentiated HUES 9 and H9 cells. Because researchers employ a variety of validated medium formulations to maintain hPSCs (Thomson et al., 1998; Chen et al., 2011), we compared the metabolic state of hESCs in murine embryonic fibroblast conditioned medium (MEF-CM) or more chemically defined, commercially available media such as Essential 8 (E8). We employed this strategy to deconvolute medium-specific metabolic pathway functions from cellular pluripotency. hESCs were maintained in each medium formulation for at least three passages. Consistent with previous observations established during the establishment of these media (Thomson et al., 1998; Chen et al., 2011), hESCs under all conditions exhibited robust expression of OCT4 (Figures 1A and 1B). Notably, we observed a more compact, flattened colony morphology of hESCs cultured in chemically defined media and a larger, non-nuclear area of hESCs cultured in MEF-CM, suggesting a difference in the quantity of cytosolic biomass between both pluripotent cells (Figure 1B). We also noted striking differences in the dry cell weight of hESCs adapted to chemically defined media, which was nearly 50% lower than that observed in MEF-CM cells (Figure 1C; Figure S2A).

To gain more insights into pathway-specific differences across these conditions, we next quantified the abundance of intracellular organic and amino acids in each hESC population. In chemically defined media, we observed consistent increases in the per-cell abundance of pyruvate (Pyr), lactate (Lac), and most tricarboxylic acid (TCA) intermediates (Figure 1D; Figure S2B) despite the smaller cell size (Figure 1C; Figure S2A). A major exception to these trends was citrate, which was present at significantly lower levels in E8 medium. Consistent with these differences, glycolytic flux in E8 was significantly higher on a per-protein basis (Figure 1E). Additionally, glutamine consumption was markedly elevated in chemically defined media, and net glutamine anaplerosis (i.e., glutamine uptake minus glutamate secretion or entry of glutamine carbon into the TCA cycle) was increased ~4-fold (Figure 1F). These results suggest that different hPSC media drive metabolic reprogramming of hESCs independent of pluripotency.

Medium-Dependent Reprogramming of Amino Acid and Redox Metabolism

The inherent redundancy of metabolic networks allows for multiple pathways and substrates to support cellular bioenergetics and biosynthesis. Indeed, the differences observed in the above metabolic characterizations suggest that intermediary metabolic fluxes are altered in hESCs cultured in MEF-CM versus chemically defined media. To investigate these changes in greater detail, we cultured HUES 9 and H9 cells in the presence of [^{13}C]glucose, [^{2}H]glucose, or [^{13}C]glutamine tracers and quantified isotopic labeling to probe central carbon metabolism (see Figure S1 for atom transition maps). With the exception of serine, the contribution of glucose carbon to glycolytic and TCA intermediates was not dramatically affected by medium choice (Figure 2A; Figure S3). On the other hand, flux of glucose through the oxidative pentose phosphate pathway (PPP) was increased 3-fold in E8 medium compared with MEF-CM (Figure 2B). To better quantify how oxidative PPP flux contributes to nicotinamide adenine dinucleotide phosphate (NADPH) regeneration, we quantified label transfer from [3-^{2}H]glucose to palmitate and performed isotopomer spectral analysis (ISA) (Lewis et al., 2014). In E8 medium, the oxidative PPP accounted for 52% ± 2% and 67% ± 1% of cytosolic NADPH pool H9 and HUES 9 hESCs, respectively (Figure 2C). Because the oxidative PPP is often upregulated in highly proliferative cells, such as tumors, to support nucleotide and fatty acid synthesis (Patra and Hay, 2014), we also performed the same tests in multiple established stable cancer cell lines. We found the contribution of PPP flux to NADPH production to be significantly higher in hESCs than that observed in all cancer cell lines tested (Figure 2C; Supplemental Experimental Procedures), even when growing cancer cells in E8 medium rather than in DMEM + fetal bovine serum (FBS) (Figure S2C).

Glutamine is another important substrate that fuels mitochondrial metabolism in proliferating cells (DeBerardinis et al., 2007; Ahn and Metallo, 2015). When culturing HUES 9 or H9 hESCs in the presence of [U-$^{13}C_5$]glutamine, we observed significant changes in the overall contribution and labeling patterns of various TCA intermediates and amino acids in MEF-CM versus E8 medium (Figure 2D; Figures S2D and S4). These data indicated that glutaminolysis was highly active in hESCs cultured on all media to support TCA cycle anaplerosis but significantly higher in defined media (Figure 2D; Figures S2D and S4). Notably, cells became cytostatic upon glutamine withdrawal (data not shown) in contrast to murine ESCs, which can

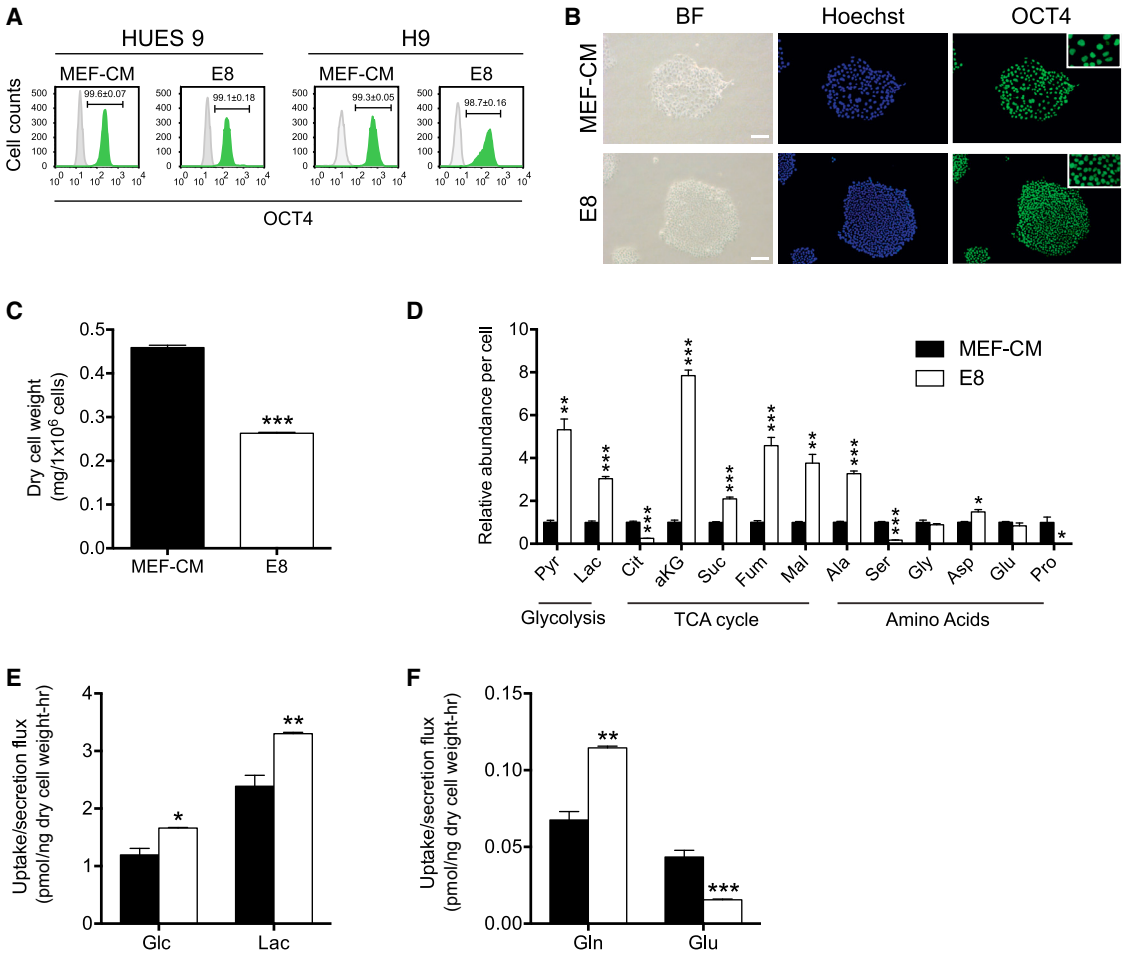

Figure 1. Distinct Metabolic States Exist in hESCs Adapted to MEF-CM versus Chemically Defined Media

HUES 9 and H9 hESCs were cultured in either MEF-CM or chemically defined media for at least three passages.

(A) Percentage of *OCT4*+ hESCs. OCT4 is shown in green and the immunoglobulin G (IgG) control in gray.

(B) Representative HUES 9 hESC colonies. The insets show increased distance between nuclei in MEF-CM cells. Scale bar, 100 μm. BF, bright field.

(C) Dry cell weight per million HUES 9 hESCs.

(D) Relative intracellular metabolite abundance of HUES 9 hESCs normalized by cell number and MEF-CM sample. Metabolite abbreviations are defined in the Supplemental Experimental Procedures.

(E) Glucose uptake and lactate secretion fluxes of HUES 9 hESCs.

(F) Glutamine uptake and glutamate secretion fluxes of HUES 9 hESCs.

(A and C–F) All results are shown as mean ± SEM.

(C–F) p values were calculated using Student's two-tailed t test relative to MEF-CM condition. *p = between 0.01 and 0.05, **p = between 0.001 and 0.01, ***p < 0.001.

proliferate in the absence of available glutamine (Carey et al., 2015). Increased M+3 labeling of citrate, malate (Mal), fumarate (Fum), and aspartate suggested that reductive carboxylation and ATP-citrate lyase activity (in the case of citrate) were both elevated in cells cultured in E8 (Figure S4). We confirmed that glutamine-mediated reductive carboxylation flux was increased in chemically defined culture media by tracing the contribution of [1-^{13}C]glutamine to various intermediates (Figure 2E). This NADPH-dependent pathway can fuel lipid biosynthesis via citrate and is particularly active under conditions of oxidative stress or hypoxia-inducible factor (HIF) stabilization (Metallo et al., 2011; Mullen et al., 2011; Wise et al., 2011; Fendt et al., 2013). In addition, we observed elevated levels of 2-hydroxyglutarate (2HG) in cells grown in chemically defined medium (Figure 2F). We confirmed this metabolite as the (R)-2HG enantiomer via chiral chromatography (Figure S2E; Supplemental Experimental Procedures), suggesting that this 2HG was produced by IDH1. However, the levels present in all conditions were significantly lower than that required for modulation of alpha-ketoglutarate (aKG)-dependent dioxygenase activity (Xu et al., 2011; Grassian et al., 2014). These results suggest that the TCA cycle, the central hub of mitochondrial oxidative energy generation, resides in distinct states within hESCs depending on the nutritional environment of cells.

Please cite this article in press as: Zhang et al., Distinct Metabolic States Can Support Self-Renewal and Lipogenesis in Human Pluripotent Stem Cells under Different Culture Conditions, Cell Reports (2016), http://dx.doi.org/10.1016/j.celrep.2016.06.102

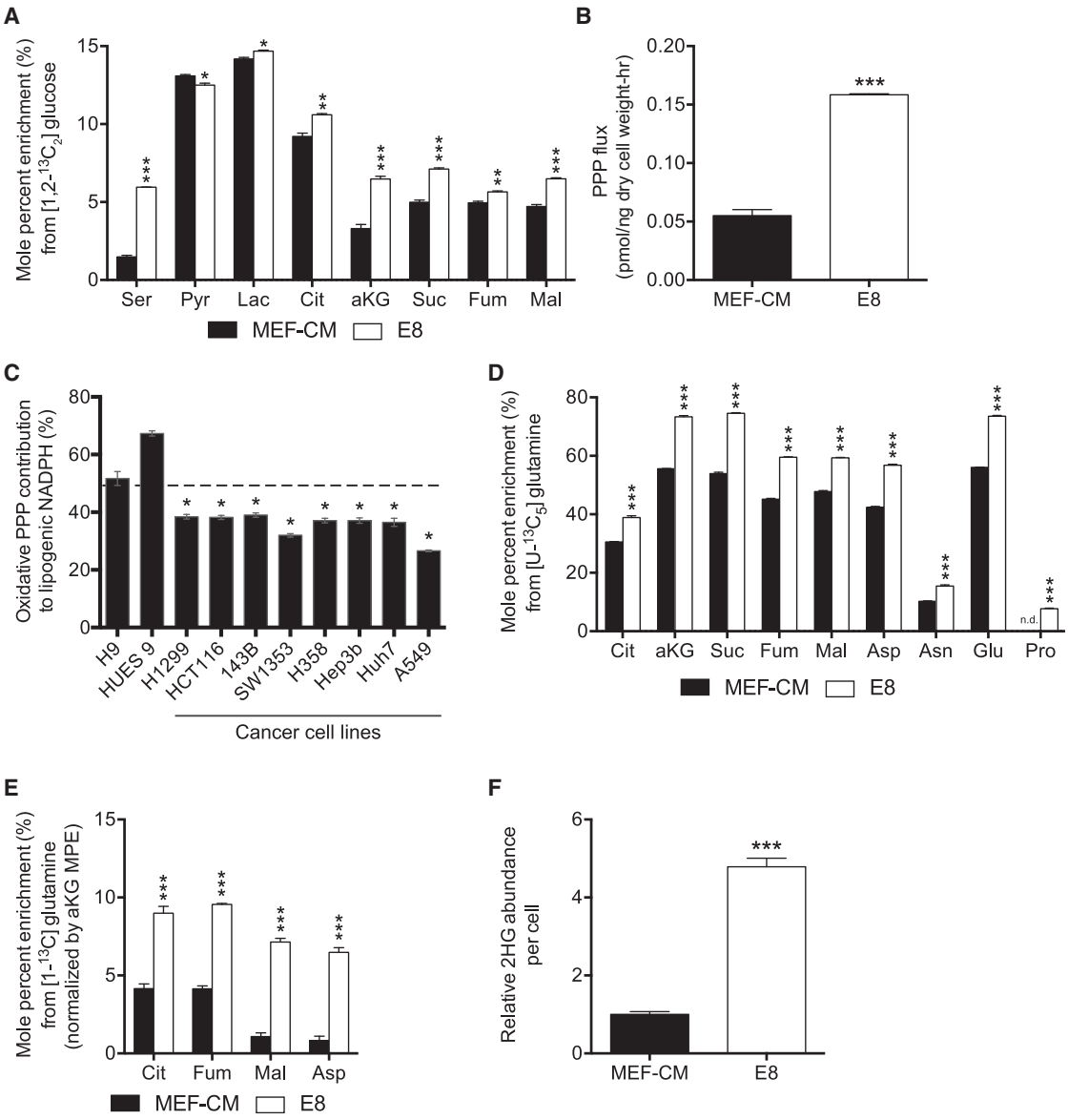

Figure 2. Medium Choice Influences Glucose, Glutamine, and NADPH Metabolism

(A) MPE from [1,2-$^{13}C_2$]glucose in HUES 9 hESCs throughout intermediary metabolism.

(B) Absolute flux through the oxidative PPP in HUES 9 hESCs.

(C) Contribution of oxidative PPP to lipogenic NADPH as determined by ISA in hESCs and cancer cells. Results are shown as mean and 95% CI. *, significance indicated by non-overlapping 95% confidence intervals.

(D) MPE from [U-$^{13}C_5$]glutamine in HUES 9 hESCs throughout intermediary metabolism.

(E) MPE of TCA intermediates from [1-^{13}C]glutamine (normalized by MPE of aKG) in HUES 9 hESCs.

(F) Relative abundance of 2HG in HUES 9 hESCs normalized by cell number and MEF-CM sample.

(A, B, and D–F) All results shown as mean ± SEM. p values were calculated using Student's two-tailed t test relative to MEF-CM condition. *p = between 0.01 and 0.05, **p = between 0.001 and 0.01, ***p < 0.001.

Chemically Defined Medium Dramatically Increases Lipogenesis

The increased reductive carboxylation and 2HG production noted above provide some mechanistic insight into why oxidative PPP flux is elevated in defined media. However, in addition to the changes in intermediary metabolism, we observed significant decreases in per-cell fatty acid abundances in HUES 9 and H9 hESCs maintained in more defined media, such as E8 and mTeSR1, versus MEF-CM (Figure 3A), consistent with our observation of decreased dry cell weight of hESCs in the latter (Figure 1C; Figure S2A). We next employed [U-$^{13}C_6$]glucose and ISA to quantify de novo lipogenesis in hESCs cultured in the

same medium panel. This analysis highlighted drastic changes in the extent to which hESCs synthesized fatty acids and cholesterol in different media. Although hESCs exhibited minimal lipogenesis in MEF-CM over 24 hr, HUES 9 and H9 cells synthesized 50%–80% of their palmitate and cholesterol in E8 or mTESR1 over the same time period (Figure 3B). Notably, the contribution of glucose to lipogenic acetyl coenzyme A (AcCoA) pools did not change appreciably in different media, consistent with glucose labeling of citrate under each condition (Figures S5A and S5B). These results demonstrate that hESCs exhibit marked differences in lipid biosynthesis when cultured in different media.

Both MEF-CM and mTeSR1 formulations contain exogenous lipid supplements (AlbuMAX and chemically defined lipid concentrate, respectively) that may support hPSC growth, although our results indicate that the levels present in mTeSR1 are insufficient. To further dissect how exogenous lipids are used and metabolized in chemically defined media, we supplemented E8 with albumin-bound [U-$^{13}C_{16}$]palmitate (U-Palm E8) as the sole source of fatty acids (Figure 3C). After 24 hr, we quantified fatty acid and TCA intermediate labeling in hESCs. No appreciable isotope enrichment was detected in citrate or other TCA metabolites (data not shown), indicating that β-oxidation is not employed by self-renewing hESCs to generate AcCoA. However, M+16 labeling of C16:0 palmitate and C18:0 stearate was observed, suggesting that exogenous fatty acids are readily utilized and elongated in hESCs cultured in chemically defined medium (Figures 3D and 3E).

The metabolic changes outlined above center around pathways associated with de novo lipogenesis, NADPH regeneration, and glutaminolysis. To better understand how cells coordinate the observed changes in metabolic flux, we quantified the expression of various enzymes catalyzing these reactions. Consistent with this metabolic shift toward lipid biosynthesis and NADPH production, we observed significant increases in the expression of *ACACA, ACLY*, *FAS*, *SCD*, *G6PD*, and *GLS2* (Figure 3F). Importantly, all of these genes (with the exception of *GLS2*) are targets of the sterol response element binding proteins (SREBPs), providing evidence that cells sense lipid deficiency and respond transcriptionally through the established SREBP pathway (Porstmann et al., 2008). Recent studies have implicated *GLS2* specifically in both antioxidant function and as being necessary for differentiation (Hu et al., 2010; Suzuki et al., 2010; Velletri et al., 2013). These results indicate that nutritional availability influences both metabolic fluxes and gene expression in hESCs.

Lipid Supplementation Mitigates hESC Metabolic Reprogramming

Our results demonstrate that hESCs in different medium compositions can self-renew in distinct metabolic states, exemplified by drastic changes in NADPH, lipid, and amino acid metabolism. More specifically, these differences suggest that insufficient lipid availability in media, including mTeSR1 and E8, drive medium-induced metabolic reprogramming, which influences metabolic rates (as indicated above) and, potentially, cellular epigenetics (Moussaieff et al., 2015). To determine whether lipids produced by irradiated MEFs drove these changes, we conditioned media in the presence of [U-$^{13}C_6$]glucose. Although glucose was readily metabolized by MEFs to citrate (Figure S5C), no appreciable accumulation of labeled lipids was observed after conditioning (Figure S5D). This finding suggests that lipids present in basal medium may support hESC growth.

The predominant lipid source in basal hESC medium is AlbuMAX within the knockout serum replacer (KSR) supplement. This reagent contains albumin, fatty acids, cholesterol, and other lipids, and, in some background media, it can improve hESC growth (Garcia-Gonzalo and Izpisúa Belmonte, 2008). To determine whether lipid supplementation in chemically defined media can mitigate the metabolic reprogramming described above, we added AlbuMAX to E8 at a final concentration of 1.6% (E8+AlbuMAX), equivalent to that present in MEF-CM. Short-term addition of AlbuMAX did not affect *OCT4* expression, although more extensive studies are required to demonstrate its ability to support long-term hPSC expansion in specific medium backgrounds (Figure S5E). Notably, AlbuMAX supplementation to E8 rescued some of the changes in intracellular metabolite levels that we observed in defined medium. Specifically, glycolytic (Pyr, Lac) and various TCA intermediates (succinate [Suc], Fum, Mal) decreased significantly, whereas levels of the lipogenic metabolite citrate and aKG were increased (Figure 4A). Only a marginal effect on glucose uptake and Lac secretion was observed (Figure S5F), presumably because of the importance of glycolysis for pluripotency (Folmes et al., 2011; Panopoulos et al., 2012; Zhu et al., 2010) and the need for continued non-essential amino acids (NEAA) biosynthesis (e.g., serine, glycine), which were not supplemented further. However, net glutamine anaplerosis decreased in HUES 9 cells after addition of AlbuMAX, as noted by the increased glutamate secretion observed (Figure S5G).

Additionally, we quantified relevant flux changes in cells cultured in lipid-supplemented E8 versus basal E8 medium. Oxidative PPP flux was significantly decreased in HUES 9 and H9 cells under these conditions (Figure 4B). Furthermore, the contribution of PPP flux to lipogenic NADPH was also decreased in these cells (Figure 4C). Less robust changes may have occurred in PPP flux in IMR90-iPSC cultures because they were maintained for an extended number of passages in lipid-deficient media prior to supplementation (Figure 4B). On the other hand, fatty acid (palmitate) and cholesterol synthesis were significantly decreased in all hPSCs upon AlbuMAX addition (Figures 4D and 4E).

Lipid supplementation also influenced the general phenotype of hPSCs. Lipid supplementation significantly decreased the transcription of most enzymes involved in de novo lipogenesis that were previously observed to be upregulated in chemically defined media, with consistent results obtained in HUES 9 and H9 hESCs as well as an IMR90-derived iPSC line (Figures 5A–5C). Additionally, per-cell dry weight increased significantly in E8+AlbuMAX HUES 9, H9, and IMR90-iPSC cultures (Figure 5D). In our hands, HUES 9 cell growth was not affected by growth in E8+AlbuMAX when additional BSA was included in the formulation. However, some growth suppression was observed in H9 and IMR90-iPS hPSCs (data not shown), indicating that additional optimization of lipid supplement background medium combinations may be needed. To more functionally characterize mitochondria under these conditions, we conducted a respirometry analysis. Basal,

Please cite this article in press as: Zhang et al., Distinct Metabolic States Can Support Self-Renewal and Lipogenesis in Human Pluripotent Stem Cells under Different Culture Conditions, Cell Reports (2016), http://dx.doi.org/10.1016/j.celrep.2016.06.102

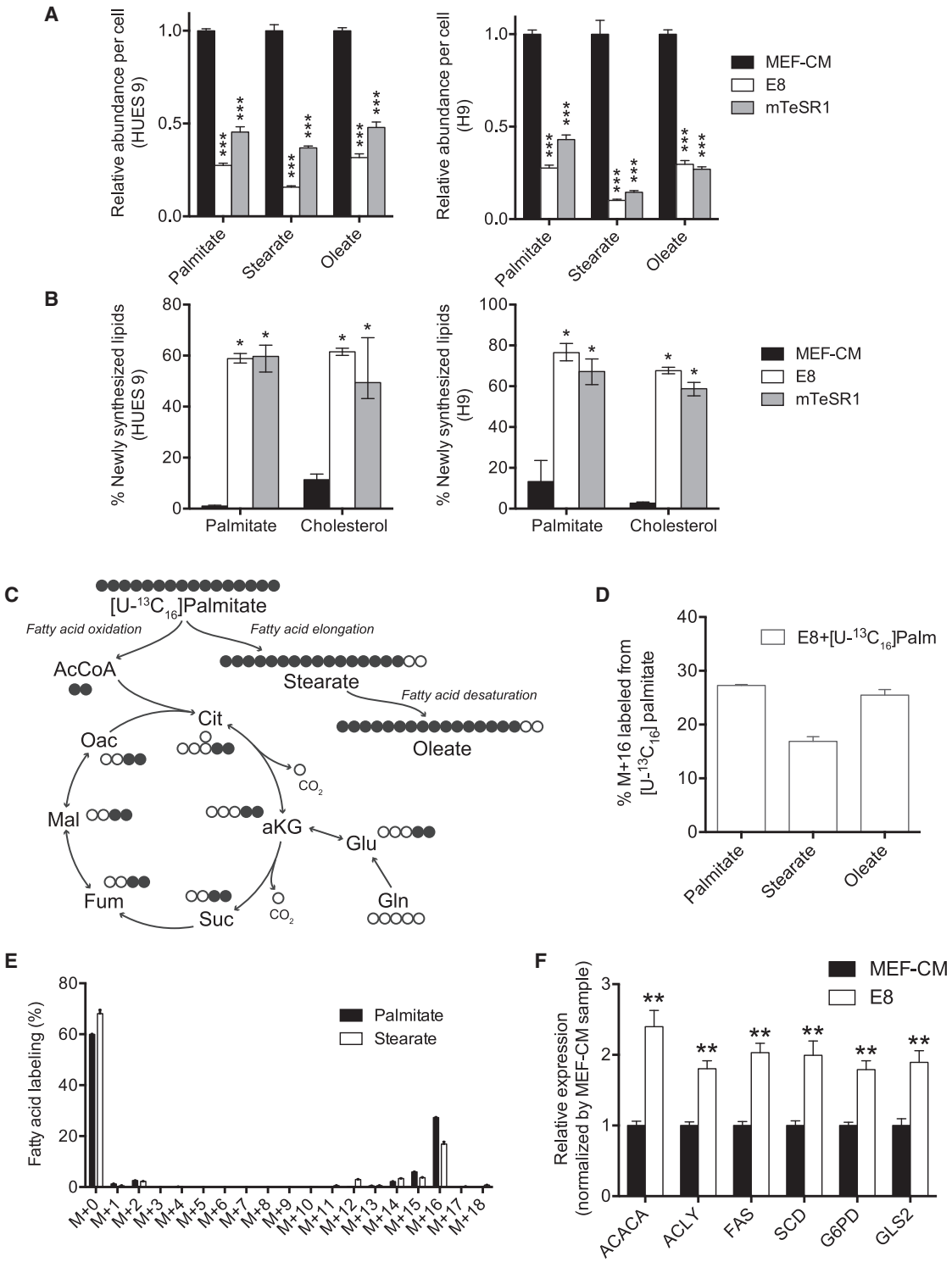

Figure 3. hESCs Adapted to Chemically Defined Media Upregulate Lipid Biosynthesis

(A) Relative fatty acid abundance in cells adapted to MEF-CM, E8, and mTeSR1 normalized by MEF-CM sample. Left and right: HUES 9 and H9 hESCs, respectively.

(B) Percentage of newly synthesized palmitate and cholesterol after 24 hr. Left and right: HUES 9 and H9 hESCs, respectively. Results are shown as mean and 95% CI. *, significance indicated by non-overlapping 95% confidence intervals.

(C) Schematic of [U-$^{13}C_{16}$]palmitate metabolism. Open circles depict ^{12}C and filled circles depict ^{13}C atoms. Metabolite abbreviations are defined in the Supplemental Experimental Procedures.

(legend continued on next page)

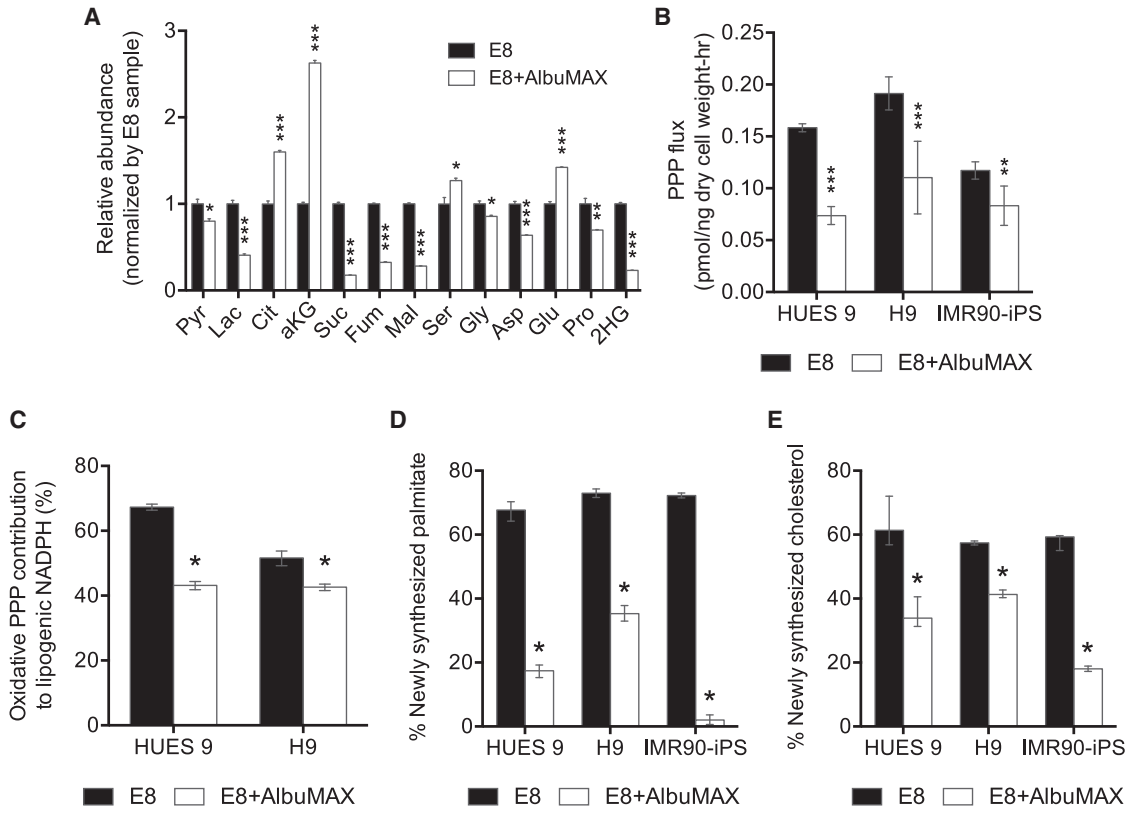

Figure 4. Lipid Supplementation Mitigates Medium-Induced Metabolic Flux Alterations

hPSCs were cultured in either E8 or E8 with 1.6% (w/v) AlbuMAX for at least three passages.

(A) Relative metabolite abundance of HUES 9 hESCs normalized by cell number and E8 sample.

(B) Absolute oxidative PPP fluxes in hPSCs.

(C) Contribution of oxidative PPP to lipogenic NADPH as determined by ISA in HUES 9 and H9 cells.

(D) Percentage of newly synthesized palmitate after 24 hr.

(E) Percentage of newly synthesized cholesterol after 24 hr.

(A and B) All results are shown as mean ± SEM. p values were calculated using Student's two-tailed t test relative to E8. *p = between 0.01 and 0.05, **p = between 0.001 and 0.01, ***p < 0.001.

(C and E) Results are shown as mean and 95% CI. *Significance indicated by non-overlapping 95% confidence intervals.

ATP-linked oxygen consumption was significantly lower in HUES 9 cells cultured in E8 compared with those maintained in MEF-CM (Figure 5E; Figure S6A). Consistent with the rescue experiments above, supplementation of AlbuMAX to E8 significantly increased the respiration of HUES 9, H9, and IMR90 iPSCs (Figure 5F; Figures S6A–S6C). Taken together, these data indicate that lipid deficiency of chemically defined media induced a profound reliance on biosynthetic fluxes because of the need for structural lipids in proliferating hESCs. In turn, this metabolic reprogramming influences the respiratory state, gene expression profile, and mitochondrial function of hPSCs. These data strongly contrast the concept of mitochondrial inactivity as a key requirement for pluripotency-associated metabolic reprogramming and illustrate the confounding effects of nutrient availability in hPSC metabolic studies.

DISCUSSION

The prevailing view of hPSC metabolism is highly reminiscent of tumor cell metabolism in that aerobic glycolysis is thought to be favored over oxidative mitochondrial metabolism (Vander Heiden et al., 2010; Zhang et al., 2012; Vacanti and Metallo, 2013; Prigione et al., 2010). These findings are supported by metabolic studies predominantly conducted in chemically defined media

(D) Percentage of M+16 fatty acids in HUES 9 hESCs cultured in E8+ BSA-bound [U-$^{13}C_{16}$]palmitate and 1 mM carnitine.

(E) Mass isotopomer distribution of palmitate and stearate in HUES 9 hESCs cultured in E8 with BSA-bound [U-$^{13}C_{16}$]palmitate and 1 mM carnitine.

(F) Expression of genes encoding various metabolic enzymes in HUES 9 hESCs adapted to E8 relative to cells in MEF-CM.

(A and D–F) All results are shown as mean ± SEM.

(A and F) p values were calculated using Student's two-tailed t test relative to MEF-CM condition. *p = between 0.01 and 0.05, **p = between 0.001 and 0.01, ***p < 0.001.

Please cite this article in press as: Zhang et al., Distinct Metabolic States Can Support Self-Renewal and Lipogenesis in Human Pluripotent Stem Cells under Different Culture Conditions, Cell Reports (2016), http://dx.doi.org/10.1016/j.celrep.2016.06.102

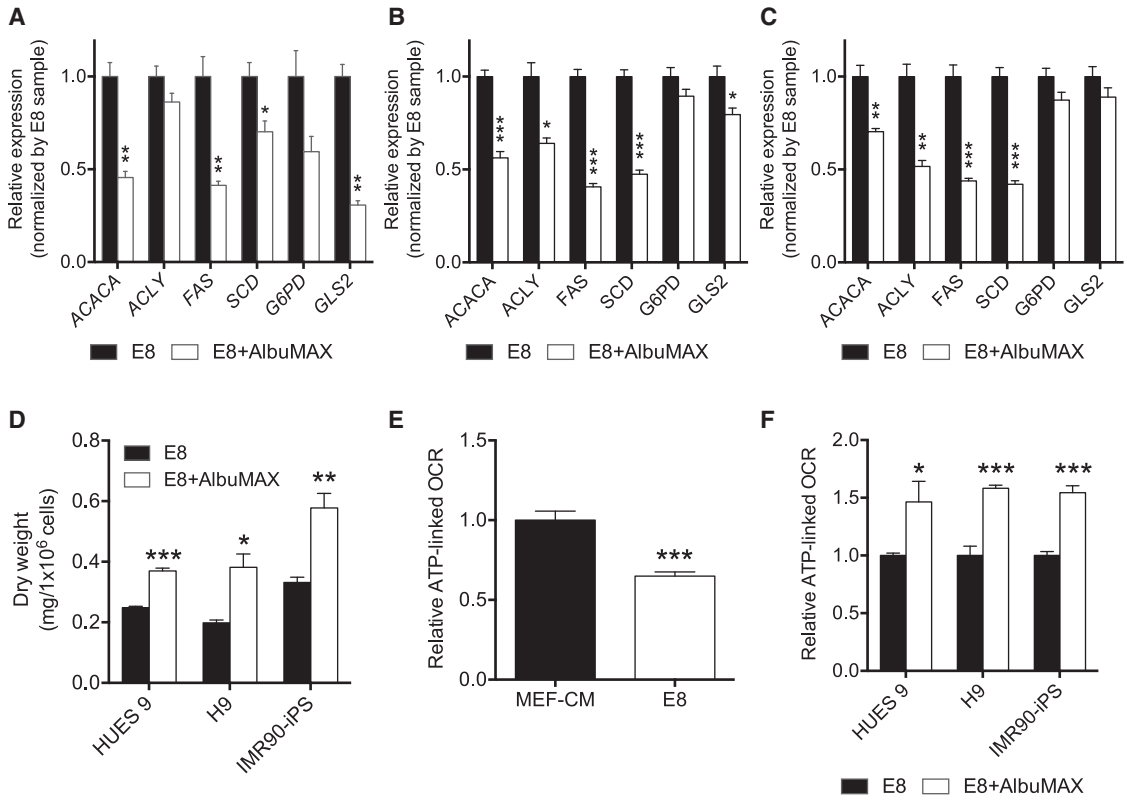

Figure 5. Lipid Supplementation Mitigates Medium-Induced Metabolic Enzyme Expression and Mitochondrial State Alterations

(A–C) Expression of genes encoding various metabolic enzymes in hPSCs adapted to E8+AlbuMAX relative to cells in E8. (A) HUES 9. (B) H9. (C) IMR90-iPS.

(D) Dry cell weight per million hPSCs.

(E) Relative ATP-linked OCR of HUES 9 hESCs in MEF-CM and E8, normalized by MEF-CM sample.

(F) Relative ATP-linked OCR of hPSCs cells in E8 and E8+AlbuMAX, normalized by E8 sample.

All results are shown as mean ± SEM. p values were calculated using Student's two-tailed t test relative to E8 condition. *p = between 0.01 and 0.05, **p = between 0.001 and 0.01, ***p < 0.001.

and/or the effect of metabolic inhibitors on reprogramming efficiency in fast-growing cultures (Folmes et al., 2011; Panopoulos et al., 2012; Zhu et al., 2010). In other studies using MEF-CM as the primary maintenance condition, metabolic analysis was limited to respirometry, with little focus on pathways involved in biosynthesis (Zhou et al., 2012; Folmes et al., 2012). Our results demonstrate that distinct metabolic states can support self-renewing hESCs when cultured under different nutrient conditions (Figure 6). In cancer biology, recent studies have shed light on the importance of mitochondria for tumor cell growth and survival as well as the potential efficacy of mitochondrial inhibitors as therapies (Viale et al., 2014; Wheaton et al., 2014). Although glycolysis similarly supports hESC growth under all conditions, our data suggest that oxidative mitochondrial metabolism is highly active in hESCs when lipids are present and sustained by glutamine anaplerosis. Amino acid availability also presumably affected serine, glycine, asparagine, and proline metabolism in our system because each of these metabolites was differentially labeled in MEF-CM and chemically defined media.

Although numerous studies have demonstrated that pluripotency and proliferation are robustly maintained in both MEF-CM and chemically defined medium alternatives (Ludwig et al., 2006; Chen et al., 2011), our metabolic flux analysis (MFA) experiments indicate that hPSCs are capable of adapting metabolism to different nutrient conditions while maintaining their self-renewal capacity. In particular, medium lipid deficiency influences the metabolic state of hESCs so that they strongly upregulate pathways involved in lipid biosynthesis and NADPH regeneration (i.e., the oxidative PPP). This metabolic state may render cells more susceptible to oxidative stresses. For example, high NADPH consumption fueling lipid synthesis in cancer cells can increase their susceptibility to metabolic or environmental stresses (Jeon et al., 2012). Additionally, glucose-6-phosphate dehydrogenase (G6PD) deficiency is a relatively common inborn error of metabolism (IEM) in the human population (Stanton, 2012). As such, mutations in G6PD may affect the efficiency of iPSC reprogramming in some populations or potentially affect the genetic stability and redox sensitivity of hPSCs cultured in chemically defined or, more specifically, lipid-free media.

hPSC applications in disease modeling, drug screening, and regenerative medicine all require the robust production of differentiated lineages that correctly recapitulate the metabolic functions of somatic tissue. Organogenesis is a complex, multistep

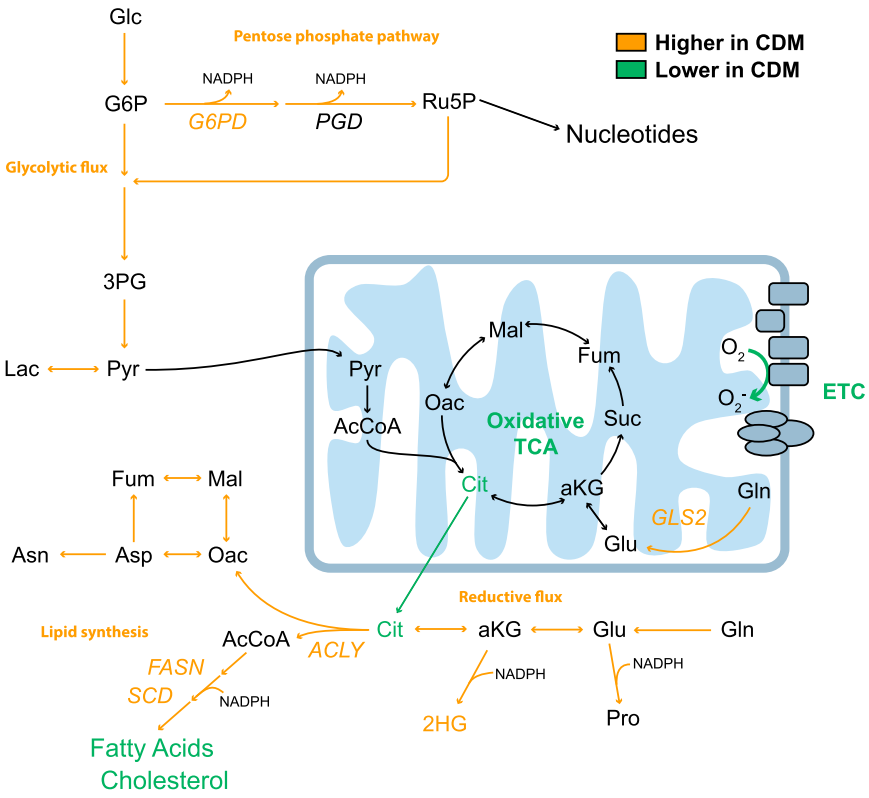

Figure 6. Nutrient Availability Reprograms Intermediary Metabolism in hPSCs

Culture of hPSCs in chemically defined media (CDM) reprograms glucose, glutamine, lipid, and NADPH metabolism. Lipid deficiency induces the upregulation of oxidative PPP flux for NADPH synthesis, de novo lipogenesis, and reductive carboxylation while diverting carbon from the TCA cycle and decreasing mitochondrial respiration (ATP-linked activity of the mitochondrial electron transport chain [ETC]). Amino acid deficiencies influence glutaminolysis and synthesis of proline, asparagine, and serine, which are upregulated in hPSCs cultured in defined media. Metabolic genes are shown in italics. Metabolite abbreviations are defined in the Supplemental Experimental Procedures.

process that requires significant energy, biomass, and signaling cues; metabolism plays an essential role in all aspects of these processes. Subjecting hPSCs to selective pressures in vitro, such as medium lipid deficiency, may limit their ability to accurately represent normal tissue function in subsequent applications without giving rise to "harmful" genetic alterations (Peterson and Loring, 2014). Furthermore, culture and passaging conditions as well as time can influence the genetic and epigenetic stability of hPSCs (Laurent et al., 2011; Garitaonandia et al., 2015) or metabolic rates after subculture (Badur et al., 2015). Our MFA results provide potential mechanisms that may be exploited to alleviate some of the stresses associated with long-term in vitro expansion. Specifically, addition of particular lipids may enhance or better control hPSC expansion and differentiation. As such, pluripotency analysis (e.g., teratoma formation) and proliferation alone may not be suitable metrics for the evaluation of hPSC culture media, and intracellular metabolic fluxes should also be considered. MFA is an ideal and underutilized tool for such applications.

Numerous studies have recently implicated metabolites or culture conditions in regulating the cellular epigenetics and differentiation propensity of pluripotent stem cells. Metabolites that affect methylation (Carey et al., 2015; Wang et al., 2009; Shiraki et al., 2014) and acetylation (Moussaieff et al., 2015) can influence differentiation but likely play more critical roles in cellular bioenergetics and biosynthesis. Indeed, it is unclear how global changes in the abundance of s-adenosyl methionine (SAM) or AcCoA can affect the specific epigenetic state of pluripotency genes. Other studies have recently identified key differences in the predisposition of cells to differentiate to neural or hematopoietic lineages when culturing or priming cells in MEF-CM versus more nutrient-limited media, such as E8 or mTeSR1 (Lee et al., 2015; Lippmann et al., 2014). Finally, the mitochondrial state and lipid profile of cells changes significantly during the course of mESC and hESC differentiation (Yanes et al., 2010). Our results therefore demonstrate the importance of considering the broader nutritional environment and intracellular metabolic state of hPSCs when characterizing metabolic regulation in stem cells and designing hPSC media.

EXPERIMENTAL PROCEDURES

hPSC Culture

The human embryonic stem cell lines HUES 9 and WA09 (H9) and the human induced pluripotent stem cell line iPS(IMR90)-c4 were maintained on plates coated with Matrigel (Corning Life Sciences) at 8.8 μg/cm^2 and adapted to MEF-CM, Essential 8 medium (Life Technologies), and mTeSR1 medium (STEMCELL Technologies) for at least three passages before experiments. All hPSCs were passaged every 5 days by exposure to Accutase (Innovative Cell Technology) for 5–10 min at 37°C. For metabolic flux experiments, 1× minimum essential medium (MEM) non-essential amino acid solution was added to E8 medium to control for amino acid levels. Tracer MEF-CM consisted of low-glucose or glutamine-free MEF-CM supplemented with either [^{13}C] glucose or [^{13}C] glutamine tracers, respectively. Tracer chemically defined medium consisted of glucose or glutamine-free E8 medium supplemented with [^{13}C] glutamine, [^{13}C] glucose or [^{2}H] glucose, or E8 medium supplemented with [^{13}C] palmitate. All tracers were purchased from Cambridge Isotopes. Additional details are described in the Supplemental Experimental Procedures. All human pluripotent cell research was approved by the University of California, San Diego (UCSD) Embryonic Stem Cell Research Oversight (ESCRO) Committee.

Immunocytochemistry

hESCs were harvested and resuspended in 1% (v/v) paraformaldehyde and then fixed in 90% cold methanol. Cell pellets were incubated with a 1:100 dilution of human OCT-3/4 primary mouse antibody (Santa Cruz Biotechnology, C-10) and a 1:1,000 dilution of the secondary antibody conjugated with Alexa Fluor 488 (Molecular Probes). The *OCT4*+ cells were detected by Becton Dickinson (BD) flow cytometry, and the results were analyzed by FlowJo. For

Please cite this article in press as: Zhang et al., Distinct Metabolic States Can Support Self-Renewal and Lipogenesis in Human Pluripotent Stem Cells under Different Culture Conditions, Cell Reports (2016), http://dx.doi.org/10.1016/j.celrep.2016.06.102

microscopy imaging, the adherent cells were fixed in 4% (v/v) paraformaldehyde. Cells were incubated with a 1:100 dilution of human OCT-3/4 primary mouse antibody and a 1:1,000 dilution of the secondary antibody conjugated with Alexa Fluor 488. Cells were subsequently washed and incubated with Hoechst 33342 nucleus staining solution.

Metabolite Extraction and Derivatization

Polar metabolites and fatty acids were extracted using methanol/water/chloroform. Briefly, spent medium was removed, and cells were rinsed with 0.9% (w/v) saline, and 250 μl of −80°C methanol was added to quench metabolism. 100 μl of ice-cold water containing 1 μg norvaline internal standard was added to each well. Both solution and cells were collected via scraping. Cell lysates were transferred to fresh sample tubes, and 250 μl of −20°C chloroform containing 1 μg heptadecanoate (internal standard for fatty acids) and 1 μg coprostan-3-ol (internal standard for cholesterol) were added. After vortexing and centrifugation, the top aqueous layer (polar metabolites) and bottom organic layer (lipids) were collected and dried under airflow. All reagents were purchased from Sigma-Aldrich.

Derivatization of polar metabolites was performed using the Gerstel Multi-Purpose Sampler (MPS 2XL). Dried polar metabolites were dissolved in 20 μl of 2% (w/v) methoxyamine hydrochloride (MP Biomedicals) in pyridine and held at 37°C for 60 min. Subsequent conversion to their tert-butyldimethylsilyl (tBDMS) derivatives was accomplished by adding 30 μl *N*-methyl-*N*-(tert-butyldimethylsilyl) trifluoroacetamide + 1% tert-butyldimethylchlorosilane (Regis Technologies) and incubating at 37°C for 30 min. Fatty acid methyl esters (FAMEs) were generated by dissolving dried fatty acids in 0.5 ml 2% (v/v) methanolic sulfuric acid (Sigma-Aldrich) and incubating at 50°C for 2 hr. FAMEs were subsequently extracted in 1 ml hexane with 0.1 ml saturated sodium chloride. FAME samples subsequently were aliquoted to two tubes for direct analysis or cholesterol derivatization. One dried FAME extract was converted to cholesterol trimethylsilyl (TMS) derivatives by adding 30 μl *N*-Methyl-*N*-(trimethylsilyl) trifluoroacetamide (Regis Technologies) and incubating at 37°C for 30 min.

Gas Chromatography/Mass Spectrometry Analysis

Gas chromatography/mass spectrometry (GC/MS) analysis was performed using an Agilent 7890A with a 30-m DB-35MS capillary column (Agilent Technologies) connected to an Agilent 5975C MS. GC/MS was operated under electron impact (EI) ionization at 70 electronvolts (eV). In splitless mode, a 1-μl sample was injected at 270°C, using helium as the carrier gas at a flow rate of 1 ml/min. For analysis of organic and amino acid derivatives, the GC oven temperature was held at 100°C for 2 min, increased to 255°C at 3.5°C/min, and then ramped to 320°C at 15°C/min for a total run time of approximately 50 min. For measurement of FAMEs, the GC oven temperature was held at 100°C for 3 min, increased to 205°C at 25°C/min, further increased to 230°C at 5°C/min, and ramped up to 300°C at 25°C/min for a total run time of approximately 15 min. For measurement of cholesterol, the GC oven temperature was held at 150°C for 1 min, increased to 260°C at 20°C/min and held for 3 min, and further increased to 280°C at 10°C/min and held for 15 min, and finally ramped up to 325°C for a total run time of approximately 30 min. The MS source and quadrupole were held at 230°C and 150°C, respectively, and the detector was operated in scanning mode, recording ion abundance in the range of 100–650 mass-to-charge ratio (m/z).

Metabolite Quantification and Isotopomer Spectral Analysis

For quantification of metabolites and mass isotopomer distributions, selected ion fragments were integrated and corrected for natural isotope abundance using an in-house, MATLAB-based algorithm and the metabolite fragments listed in Table S1. Total abundances were normalized by counts of internal standard control. ISA for quantitation of [1,2-$^{13}C_2$] glucose and [U-$^{13}C_6$] glucose contribution to lipogenic AcCoA and [3-^{2}H] glucose contribution to lipogenic NADPH were calculated as described previously (Vacanti et al., 2014; Lewis et al., 2014). Specifically, the relative enrichment of the lipogenic AcCoA and NADPH pools from a given tracer and the percentage of newly synthesized fatty acids were estimated from a best fit model using the isotopomer network compartmental analysis (INCA) MFA software package (Young, 2014). The 95% confidence intervals (CIs) for both parameters were determined by evaluating the sensitivity of the sum of squared residuals between measured and simulated palmitate mass isotopomer distributions to small flux variations (Antoniewicz et al., 2006).

Mole Percent Enrichment Measurement

Mole percent enrichment (MPE) of isotopes was calculated as the percent of all atoms within the metabolite pool that are labeled

$$\frac{\sum_{i=1}^{n} M_i \cdot i}{n},$$

where n is the number of carbon atoms in the metabolite and M_i is the relative abundance of the i^{th} mass isotopomer.

Extracellular Flux and Oxidative Pentose Phosphate Pathway Flux Measurements

Per-dry cell weight extracellular fluxes, including glucose/glutamine uptake and Lac/glutamate secretion, were calculated by subtracting final spent medium from initial medium substrate concentrations measured using a Yellow Springs Instrument 2950 and normalized by the integral dry weights of hPSCs over 24 hr (Vacanti et al., 2014). Quantification of oxidative PPP flux was determined by extracellular glucose uptake flux times the ratio of

$$\frac{M+1}{(M+1)+(M+2)},$$

where (M + 1) and (M + 2) are the isotopologues of Pyr derived from [1,2-$^{13}C_2$] glucose.

Cell Dry Weight Measurements

hPSCs were harvested and counted at 90% confluence. Cell pellets were dried by ambient air at 50°C for 3 days. Total weights of cell pellets were then measured, and weight per million cells was calculated.

ATP-Linked Oxygen Consumption Rate Measurements

Respiration was measured in viable hPSCs using a Seahorse XF96 analyzer. hPSCs were assayed in fresh culture media. The ATP-linked oxygen consumption rate (OCR) was calculated as the oxygen consumption rate sensitive to 2 mg/ml oligomycin under each culture condition and normalized by cell abundance. Each culture condition sample had at least four biological replicates analyzed. Cell abundance was indicated by the total fluorescence after staining with Hoechst 33342 (Divakaruni et al., 2014).

Gene Expression Analysis

Total mRNA was isolated from 75% confluent hPSCs using an RNA isolation kit (RNeasy mini kit, QIAGEN). Isolated RNA was reverse-transcribed using a cDNA synthesis kit (iScipt Reverse Transcription Supermix, Bio-Rad). Real-time PCR was performed using SYBR Green reagent (iTaq Universal SYBR Green Supermix, Bio-Rad). Relative expression was determined using the Livak ($\Delta\Delta C_T$) method with *GAPDH* as the housekeeping gene. The primers used were taken from Primerbank (Wang et al., 2012) and tabulated in Table S2. All commercial kits were used according to the manufacturer's protocol.

Statistical Analyses

All results shown are as averages of triplicates (at least) and presented as mean ± SEM. p values were calculated using Student's two-tailed t test (*p = between 0.01 and 0.05, **p = between 0.001 and 0.01, ***p < 0.001). All errors associated with ISA were 95% confidence intervals determined via confidence interval analysis.

SUPPLEMENTAL INFORMATION

Supplemental Information includes Supplemental Experimental Procedures, six figures, and two tables and can be found with this article online at http://dx.doi.org/10.1016/j.celrep.2016.06.102.

AUTHOR CONTRIBUTIONS

H.Z., M.G.B., and C.M.M. designed the study. H.Z., M.G.B., A.S.D., A.N.M., S.J.P., C.J., and K.H. carried out the experiments and analyzed the data. H.Z., M.G.B., and C.M.M. wrote the manuscript, and all authors read the paper.

ACKNOWLEDGMENTS

HUES 9 hESCs were provided by Prof. Shyni Varghese (University of California, San Diego). H9 hESCs and IMR90 iPSCs were provided by Prof. Sean Palecek (University of Wisconsin, Madison). The authors acknowledge Yongsung Hwang, Shyni Varghese, and members of the C.M.M. lab for technical assistance and helpful discussions. This research was supported by California Institute of Regenerative Medicine grant RB5-07356, NIH grant R01CA188652, a Searle Scholar Award (to C.M.M.), NSF CAREER Award 1454425 (to C.M.M.), and NSF Graduate Research Fellowship DGE-1144086 (to M.G.B.).

Received: September 18, 2015
Revised: May 20, 2016
Accepted: June 30, 2016
Published: July 28, 2016

REFERENCES

Ahn, C.S., and Metallo, C.M. (2015). Mitochondria as biosynthetic factories for cancer proliferation. Cancer Metab. *3*, 1.

Antoniewicz, M.R., Kelleher, J.K., and Stephanopoulos, G. (2006). Determination of confidence intervals of metabolic fluxes estimated from stable isotope measurements. Metab. Eng. *8*, 324–337.

Badur, M.G., Zhang, H., and Metallo, C.M. (2015). Enzymatic passaging of human embryonic stem cells alters central carbon metabolism and glycan abundance. Biotechnol. J. *10*, 1600–1611.

Ben-Zvi, D., and Melton, D.A. (2015). Modeling human nutrition using human embryonic stem cells. Cell *161*, 12–17.

Carey, B.W., Finley, L.W., Cross, J.R., Allis, C.D., and Thompson, C.B. (2015). Intracellular α-ketoglutarate maintains the pluripotency of embryonic stem cells. Nature *518*, 413–416.

Carpenter, M.K., and Couture, L.A. (2010). Regulatory considerations for the development of autologous induced pluripotent stem cell therapies. Regen. Med. *5*, 569–579.

Chen, G., Gulbranson, D.R., Hou, Z., Bolin, J.M., Ruotti, V., Probasco, M.D., Smuga-Otto, K., Howden, S.E., Diol, N.R., Propson, N.E., et al. (2011). Chemically defined conditions for human iPSC derivation and culture. Nat. Methods *8*, 424–429.

DeBerardinis, R.J., Mancuso, A., Daikhin, E., Nissim, I., Yudkoff, M., Wehrli, S., and Thompson, C.B. (2007). Beyond aerobic glycolysis: transformed cells can engage in glutamine metabolism that exceeds the requirement for protein and nucleotide synthesis. Proc. Natl. Acad. Sci. USA *104*, 19345–19350.

Desai, N., Rambhia, P., and Gishto, A. (2015). Human embryonic stem cell cultivation: historical perspective and evolution of xeno-free culture systems. Reprod. Biol. Endocrinol. *13*, 9.

Divakaruni, A.S., Paradyse, A., Ferrick, D.A., Murphy, A.N., and Jastroch, M. (2014). Analysis and interpretation of microplate-based oxygen consumption and pH data. Methods Enzymol. *547*, 309–354.

Fendt, S.M., Bell, E.L., Keibler, M.A., Olenchock, B.A., Mayers, J.R., Wasylenko, T.M., Vokes, N.I., Guarente, L., Vander Heiden, M.G., and Stephanopoulos, G. (2013). Reductive glutamine metabolism is a function of the α-ketoglutarate to citrate ratio in cells. Nat. Commun. *4*, 2236.

Folmes, C.D., Nelson, T.J., Martinez-Fernandez, A., Arrell, D.K., Lindor, J.Z., Dzeja, P.P., Ikeda, Y., Perez-Terzic, C., and Terzic, A. (2011). Somatic oxidative bioenergetics transitions into pluripotency-dependent glycolysis to facilitate nuclear reprogramming. Cell Metab. *14*, 264–271.

Folmes, C.D., Dzeja, P.P., Nelson, T.J., and Terzic, A. (2012). Metabolic plasticity in stem cell homeostasis and differentiation. Cell Stem Cell *11*, 596–606.

Garcia-Gonzalo, F.R., and Izpisúa Belmonte, J.C. (2008). Albumin-associated lipids regulate human embryonic stem cell self-renewal. PLoS ONE *3*, e1384.

Garitaonandia, I., Amir, H., Boscolo, F.S., Wambua, G.K., Schultheisz, H.L., Sabatini, K., Morey, R., Waltz, S., Wang, Y.C., Tran, H., et al. (2015). Increased risk of genetic and epigenetic instability in human embryonic stem cells associated with specific culture conditions. PLoS ONE *10*, e0118307.

Grassian, A.R., Parker, S.J., Davidson, S.M., Divakaruni, A.S., Green, C.R., Zhang, X., Slocum, K.L., Pu, M., Lin, F., Vickers, C., et al. (2014). IDH1 mutations alter citric acid cycle metabolism and increase dependence on oxidative mitochondrial metabolism. Cancer Res. *74*, 3317–3331.

Hu, W., Zhang, C., Wu, R., Sun, Y., Levine, A., and Feng, Z. (2010). Glutaminase 2, a novel p53 target gene regulating energy metabolism and antioxidant function. Proc. Natl. Acad. Sci. USA *107*, 7455–7460.

Hyun, I., Lindvall, O., Ahrlund-Richter, L., Cattaneo, E., Cavazzana-Calvo, M., Cossu, G., De Luca, M., Fox, I.J., Gerstle, C., Goldstein, R.A., et al. (2008). New ISSCR guidelines underscore major principles for responsible translational stem cell research. Cell Stem Cell *3*, 607–609.

Jeon, S.M., Chandel, N.S., and Hay, N. (2012). AMPK regulates NADPH homeostasis to promote tumour cell survival during energy stress. Nature *485*, 661–665.

Kirouac, D.C., and Zandstra, P.W. (2008). The systematic production of cells for cell therapies. Cell Stem Cell *3*, 369–381.

Laurent, L.C., Ulitsky, I., Slavin, I., Tran, H., Schork, A., Morey, R., Lynch, C., Harness, J.V., Lee, S., Barrero, M.J., et al. (2011). Dynamic changes in the copy number of pluripotency and cell proliferation genes in human ESCs and iPSCs during reprogramming and time in culture. Cell Stem Cell *8*, 106–118.

Lee, J.B., Graham, M., Collins, T.J., Lee, J.H., Hong, S.H., Mcnicol, A.J., Shapovalova, Z., and Bhatia, M. (2015). Reversible lineage-specific priming of human embryonic stem cells can be exploited to optimize the yield of differentiated cells. Stem Cells *33*, 1142–1152.

Lewis, C.A., Parker, S.J., Fiske, B.P., McCloskey, D., Gui, D.Y., Green, C.R., Vokes, N.I., Feist, A.M., Vander Heiden, M.G., and Metallo, C.M. (2014). Tracing compartmentalized NADPH metabolism in the cytosol and mitochondria of mammalian cells. Mol. Cell *55*, 253–263.

Lippmann, E.S., Estevez-Silva, M.C., and Ashton, R.S. (2014). Defined human pluripotent stem cell culture enables highly efficient neuroepithelium derivation without small molecule inhibitors. Stem Cells *32*, 1032–1042.

Ludwig, T.E., Bergendahl, V., Levenstein, M.E., Yu, J., Probasco, M.D., and Thomson, J.A. (2006). Feeder-independent culture of human embryonic stem cells. Nat. Methods *3*, 637–646.

Metallo, C.M., Gameiro, P.A., Bell, E.L., Mattaini, K.R., Yang, J., Hiller, K., Jewell, C.M., Johnson, Z.R., Irvine, D.J., Guarente, L., et al. (2011). Reductive glutamine metabolism by IDH1 mediates lipogenesis under hypoxia. Nature *481*, 380–384.

Moussaieff, A., Rouleau, M., Kitsberg, D., Cohen, M., Levy, G., Barasch, D., Nemirovski, A., Shen-Orr, S., Laevsky, I., Amit, M., et al. (2015). Glycolysis-mediated changes in acetyl-CoA and histone acetylation control the early differentiation of embryonic stem cells. Cell Metab. *21*, 392–402.

Mullen, A.R., Wheaton, W.W., Jin, E.S., Chen, P.H., Sullivan, L.B., Cheng, T., Yang, Y., Linehan, W.M., Chandel, N.S., and DeBerardinis, R.J. (2011). Reductive carboxylation supports growth in tumour cells with defective mitochondria. Nature *481*, 385–388.

Panopoulos, A.D., Yanes, O., Ruiz, S., Kida, Y.S., Diep, D., Tautenhahn, R., Herrerías, A., Batchelder, E.M., Plongthongkum, N., Lutz, M., et al. (2012). The metabolome of induced pluripotent stem cells reveals metabolic changes occurring in somatic cell reprogramming. Cell Res. *22*, 168–177.

Patra, K.C., and Hay, N. (2014). The pentose phosphate pathway and cancer. Trends Biochem. Sci. *39*, 347–354.

Peterson, S.E., and Loring, J.F. (2014). Genomic instability in pluripotent stem cells: implications for clinical applications. J. Biol. Chem. *289*, 4578–4584.

Please cite this article in press as: Zhang et al., Distinct Metabolic States Can Support Self-Renewal and Lipogenesis in Human Pluripotent Stem Cells under Different Culture Conditions, Cell Reports (2016), http://dx.doi.org/10.1016/j.celrep.2016.06.102

Porstmann, T., Santos, C.R., Griffiths, B., Cully, M., Wu, M., Leevers, S., Griffiths, J.R., Chung, Y.L., and Schulze, A. (2008). SREBP activity is regulated by mTORC1 and contributes to Akt-dependent cell growth. Cell Metab. *8*, 224–236.

Prigione, A., Fauler, B., Lurz, R., Lehrach, H., and Adjaye, J. (2010). The senescence-related mitochondrial/oxidative stress pathway is repressed in human induced pluripotent stem cells. Stem Cells *28*, 721–733.

Shiraki, N., Shiraki, Y., Tsuyama, T., Obata, F., Miura, M., Nagae, G., Aburatani, H., Kume, K., Endo, F., and Kume, S. (2014). Methionine metabolism regulates maintenance and differentiation of human pluripotent stem cells. Cell Metab. *19*, 780–794.

Shyh-Chang, N., Locasale, J.W., Lyssiotis, C.A., Zheng, Y., Teo, R.Y., Ratanasirintrawoot, S., Zhang, J., Onder, T., Unternaehrer, J.J., Zhu, H., et al. (2013). Influence of threonine metabolism on S-adenosylmethionine and histone methylation. Science *339*, 222–226.

Stanton, R.C. (2012). Glucose-6-phosphate dehydrogenase, NADPH, and cell survival. IUBMB Life *64*, 362–369.

Suzuki, S., Tanaka, T., Poyurovsky, M.V., Nagano, H., Mayama, T., Ohkubo, S., Lokshin, M., Hosokawa, H., Nakayama, T., Suzuki, Y., et al. (2010). Phosphate-activated glutaminase (GLS2), a p53-inducible regulator of glutamine metabolism and reactive oxygen species. Proc. Natl. Acad. Sci. USA *107*, 7461–7466.

Takahashi, K., and Yamanaka, S. (2006). Induction of pluripotent stem cells from mouse embryonic and adult fibroblast cultures by defined factors. Cell *126*, 663–676.

Thomson, J.A., Itskovitz-Eldor, J., Shapiro, S.S., Waknitz, M.A., Swiergiel, J.J., Marshall, V.S., and Jones, J.M. (1998). Embryonic stem cell lines derived from human blastocysts. Science *282*, 1145–1147.

Ungrin, M., O'connor, M., Eaves, C., and Zandstra, P.W. (2007). Phenotypic analysis of human embryonic stem cells. Curr. Protoc. Stem Cell Biol. *Chapter 1*, Unit 1B.3.

Vacanti, N.M., and Metallo, C.M. (2013). Exploring metabolic pathways that contribute to the stem cell phenotype. Biochim. Biophys. Acta *1830*, 2361–2369.

Vacanti, N.M., Divakaruni, A.S., Green, C.R., Parker, S.J., Henry, R.R., Ciaraldi, T.P., Murphy, A.N., and Metallo, C.M. (2014). Regulation of substrate utilization by the mitochondrial pyruvate carrier. Mol. Cell *56*, 425–435.

Vander Heiden, M.G., Locasale, J.W., Swanson, K.D., Sharfi, H., Heffron, G.J., Amador-Noguez, D., Christofk, H.R., Wagner, G., Rabinowitz, J.D., Asara, J.M., and Cantley, L.C. (2010). Evidence for an alternative glycolytic pathway in rapidly proliferating cells. Science *329*, 1492–1499.

Velletri, T., Romeo, F., Tucci, P., Peschiaroli, A., Annicchiarico-Petruzzelli, M., Niklison-Chirou, M.V., Amelio, I., Knight, R.A., Mak, T.W., Melino, G., and Agostini, M. (2013). GLS2 is transcriptionally regulated by p73 and contributes to neuronal differentiation. Cell Cycle *12*, 3564–3573.

Viale, A., Pettazzoni, P., Lyssiotis, C.A., Ying, H., Sánchez, N., Marchesini, M., Carugo, A., Green, T., Seth, S., Giuliani, V., et al. (2014). Oncogene ablation-resistant pancreatic cancer cells depend on mitochondrial function. Nature *514*, 628–632.

Villa-Diaz, L.G., Ross, A.M., Lahann, J., and Krebsbach, P.H. (2013). Concise review: The evolution of human pluripotent stem cell culture: from feeder cells to synthetic coatings. Stem Cells *31*, 1–7.

Wang, J., Alexander, P., Wu, L., Hammer, R., Cleaver, O., and McKnight, S.L. (2009). Dependence of mouse embryonic stem cells on threonine catabolism. Science *325*, 435–439.

Wang, X., Spandidos, A., Wang, H., and Seed, B. (2012). PrimerBank: a PCR primer database for quantitative gene expression analysis, 2012 update. Nucleic Acids Res. *40*, D1144–D1149.

Wheaton, W.W., Weinberg, S.E., Hamanaka, R.B., Soberanes, S., Sullivan, L.B., Anso, E., Glasauer, A., Dufour, E., Mutlu, G.M., Budigner, G.S., and Chandel, N.S. (2014). Metformin inhibits mitochondrial complex I of cancer cells to reduce tumorigenesis. eLife *3*, e02242.

Wise, D.R., Ward, P.S., Shay, J.E., Cross, J.R., Gruber, J.J., Sachdeva, U.M., Platt, J.M., DeMatteo, R.G., Simon, M.C., and Thompson, C.B. (2011). Hypoxia promotes isocitrate dehydrogenase-dependent carboxylation of α-ketoglutarate to citrate to support cell growth and viability. Proc. Natl. Acad. Sci. USA *108*, 19611–19616.

Xu, W., Yang, H., Liu, Y., Yang, Y., Wang, P., Kim, S.H., Ito, S., Yang, C., Wang, P., Xiao, M.T., et al. (2011). Oncometabolite 2-hydroxyglutarate is a competitive inhibitor of α-ketoglutarate-dependent dioxygenases. Cancer Cell *19*, 17–30.

Yanes, O., Clark, J., Wong, D.M., Patti, G.J., Sánchez-Ruiz, A., Benton, H.P., Trauger, S.A., Desponts, C., Ding, S., and Siuzdak, G. (2010). Metabolic oxidation regulates embryonic stem cell differentiation. Nat. Chem. Biol. *6*, 411–417.

Young, J.D. (2014). INCA: a computational platform for isotopically non-stationary metabolic flux analysis. Bioinformatics *30*, 1333–1335.

Zhang, J., Khvorostov, I., Hong, J.S., Oktay, Y., Vergnes, L., Nuebel, E., Wahjudi, P.N., Setoguchi, K., Wang, G., Do, A., et al. (2011). UCP2 regulates energy metabolism and differentiation potential of human pluripotent stem cells. EMBO J. *30*, 4860–4873.

Zhang, J., Nuebel, E., Daley, G.Q., Koehler, C.M., and Teitell, M.A. (2012). Metabolic regulation in pluripotent stem cells during reprogramming and self-renewal. Cell Stem Cell *11*, 589–595.

Zhou, W., Choi, M., Margineantu, D., Margaretha, L., Hesson, J., Cavanaugh, C., Blau, C.A., Horwitz, M.S., Hockenbery, D., Ware, C., and Ruohola-Baker, H. (2012). HIF1α induced switch from bivalent to exclusively glycolytic metabolism during ESC-to-EpiSC/hESC transition. EMBO J. *31*, 2103–2116.

Zhu, S., Li, W., Zhou, H., Wei, W., Ambasudhan, R., Lin, T., Kim, J., Zhang, K., and Ding, S. (2010). Reprogramming of human primary somatic cells by OCT4 and chemical compounds. Cell Stem Cell *7*, 651–655.